523-34
189683
N94-14768

Stochastic modeling of turbulent reacting flows

By R. O. Fox[1], J. C. Hill[2], F. Gao[3], R. D. Moser[4], AND M. M. Rogers[4]

Direct numerical simulations of a single-step irreversible chemical reaction with non-premixed reactants in forced isotropic turbulence at $R_\lambda = 63$, $Da = 4.0$, and $Sc = 0.7$ were made using 128^3 Fourier modes to obtain joint pdfs and other statistical information to parameterize and test a Fokker-Planck turbulent mixing model. Preliminary results indicate that the modeled gradient stretching term for an inert scalar is independent of the initial conditions of the scalar field. The conditional pdf of scalar gradient magnitudes is found to be a function of the scalar until the reaction is largely completed. Alignment of concentration gradients with local strain rate and other features of the flow were also investigated.

1. Introduction

Modern treatments of the theory of chemically reacting turbulent flows are often based on the probability density function (pdf) method, since in the pdf equations for the concentrations of the chemical species, the chemical reaction terms are closed in the statistical sense (O'Brien 1980, Pope, 1985). However, the mixing terms involving molecular diffusion are not closed, so statistical models are needed for these terms. The shortcomings of the commonly used coalescence-dispersion models and LMSE closures have been well-documented (Kosály & Givi, 1987, Leonard & Hill, 1991), and more recent closures such as the mapping closure (Chen *et al.* 1989, Pope 1991, Gao 1991) and the linear-eddy model (Kerstein 1991) are being investigated.

In the present study, the Fokker-Planck (FP) closure is applied to the joint scalar-scalar gradient pdf for a two-species, single-step, irreversible chemical reaction

$$A + B \rightarrow \text{Products} \tag{1}$$

of non-premixed reactants in forced, homogeneous isotropic turbulence. The mass conservation equation for the concentration of reactant A (ϕ_A) is

$$\frac{\partial \phi_A}{\partial t} + u_i \frac{\partial \phi_A}{\partial x_i} = D \frac{\partial^2 \phi_A}{\partial x_i \partial x_i} - S_A, \tag{2}$$

1 Kansas State University
2 Iowa State University
3 Center for Turbulence Research
4 NASA Ames Research Center

where $S_A = -k\phi_A\phi_B$ in the work described here (a similar equation described the concentration of species B). In the current development, it is assumed that the scalar diffusivity D is the same for both reactants and the product of reaction and that all physical properties are constant, including the finite reaction rate constant, k. The joint pdf's of the reactant concentrations and their gradients are used in the model discussed here to avoid problems common with closures based on pdfs of the reactant concentrations alone.

The joint pdf equation for the scalars ϕ_A and ϕ_B and their gradients ψ_A and ψ_B may be written

$$\begin{aligned}\frac{\partial P(\phi_A,\phi_B)}{\partial t} = &-\frac{\partial}{\partial\phi_A}[S_A P] - \frac{\partial}{\partial\phi_B}[S_B P] \\ &- D\frac{\partial^2}{\partial\phi_A^2}\left[\langle\psi_A^2|\phi_A,\phi_B\rangle P\right] - D\frac{\partial^2}{\partial\phi_B^2}\left[\langle\psi_B^2|\phi_A,\phi_B\rangle P\right] \\ &- 2D\frac{\partial^2}{\partial\phi_A\partial\phi_B}\left[\langle\psi_{Ai}\psi_{Bi}|\phi_A,\phi_B\rangle P\right]\end{aligned} \tag{3}$$

$$\begin{aligned}\frac{\partial P(\phi_A,\phi_B,\psi_A,\psi_B)}{\partial t} = &-\frac{\partial}{\partial\phi_A}[S_A P] - \frac{\partial}{\partial\phi_B}[S_B P] \\ &- \frac{\partial}{\partial\psi_{Ai}}\left[\frac{\partial S_A}{\partial\phi_A}\psi_{Ai}P\right] - \frac{\partial}{\partial\psi_{Bi}}\left[\frac{\partial S_B}{\partial\phi_B}\psi_{Bi}P\right] \\ &- \text{Molecular mixing terms} \\ &- \frac{\partial}{\partial\psi_{Ai}}\left[\langle d_{ij}|\phi_A,\phi_B,\psi_A,\psi_B\rangle\psi_{Ai}P\right] \\ &- \frac{\partial}{\partial\psi_{Bi}}\left[\langle d_{ij}|\phi_A,\phi_B,\psi_A,\psi_B\rangle\psi_{Bi}P\right]\end{aligned} \tag{4}$$

where $P(\ )$ is the probability density function of its arguments and the arguments to P on the right hand side of each equation are the same as those appearing on the left, S_A and S_B are the reaction source terms (both equal to $-k\phi_A\phi_B$ in this work), $d_{ij} = \partial u_i/\partial x_j$ is the velocity derivative tensor, and the summation convention applies to repeated indices. Clearly, the reaction terms in the above equations are closed. In the traditional scalar pdf formulation involving only concentrations ϕ, the three mixing terms in (3) must be modeled. In the joint pdf formulation studied here, the modeling is postponed to the gradient pdf equation (4), wherein the three molecular mixing terms (not shown) must be modeled as well as the scalar gradient magnification terms, the last two terms in (4). In the development to follow, the FP model studied here is further simplified by considering only a passive progress variable ϕ rather than both reactant concentrations and by treating the diffusion/reaction zones between the two reactants as locally one-dimensional. Among other things, this allows us to consider the magnitude of the scalar gradient $|\psi|$ rather than the full gradient vector.

In this work, we compare the results of stochastic simulations with results from direct numerical simulations (DNS) and sample the DNS results to evaluate various

quantities that appear in the pdf equations. Also, the computed fields were probed for physical insights suggested from previous simulations at lower Reynolds number (Leonard *et al.* 1988 and Leonard & Hill 1988, 1990, 1992).

2. Approach

2.1. Direct numerical simulations

To provide data to check the FP model, a direct numerical simulation of stationary, isotropic turbulence with chemically reacting scalars was carried out using the Rogallo (1981) method with 128^3 Fourier modes and low-wavenumber negative viscosity to provide the forcing. The turbulence was allowed to evolve until it reached statistical equilibrium, at which time scalar fields for the reactant concentrations were initialized and the simulations were continued. Two sets of reacting scalar initial conditions were used in the simulation. Case I was begun from "blob" initial conditions in which the two reactants are segregated into three-dimensional "blobs" with thin diffusion zones between them. The distribution of blobs was determined from a passive scalar field using a method similar to that used by Eswaran & Pope (1988). However, in this case, we follow Leonard & Hill (1991) and use a passive scalar field that has evolved with the turbulence so that the initial blobs are correlated with the velocity field. Case II uses 'slab' conditions, in which the reactants A and B are segregated into "slabs" with two planar (x–z planes) diffusion zones between them in the periodic domain. In both cases, the overall (average) reactant concentrations were in stoichiometric proportions. The Damköhler number or dimensionless reaction rate coefficient was set at $Da \equiv kA_0q^2/\epsilon = 4.0$ where $q^2 \equiv \langle u_iu_i \rangle$ and ϵ is the dissipation rate of the turbulent kinetic energy $2\nu\langle e_{ij}e_{ij}\rangle$ (e_{ij} is the strain rate tensor). The Schmidt number Sc was 0.7 for all species. The simulations were carried out until $t\epsilon/q^2 = 0.968$. Figure 1 shows the reaction zones in the plane $z = 0$ at time $t\epsilon/q^2 = 0.968$ for the two cases, showing the nearly isotropic scalar field for the blob conditions and remnants of the initial dual reaction zones in the slab case.

Comprehensive diagnostics of the simulated fields were generated, including marginal, joint, and conditional pdf's of the concentrations of the reactants and the conserved scalar $\phi = \phi_A - \phi_B$, the magnitudes of their gradients, velocity field properties such as the vorticity and dissipation, and various correlations.

2.2. Gradient alignment analysis

An analysis of the alignment of the reactant concentration gradients was carried out to provide theoretical support for stochastic models and closures that assume one-dimensionality or alignment of scalar gradients in non-premixed systems (this includes flamelet models, conditional moment closures, and the linear eddy model as well as the model developed here). The approach taken was to use (2) to obtain an expression for the evolution of the cosine of the angle μ_{AB} between scalar gradient vectors ψ_A and ψ_B, where $\mu_{AB} = \psi_{Ai}\psi_{Bi}/(|\psi_A||\psi_B|)$. For cases in which $D\mu/Dt = 0$, a linear stability analysis was performed to determine the stability of this state. General results were obtained for arbitrary reaction rate functions $S(\phi)$,

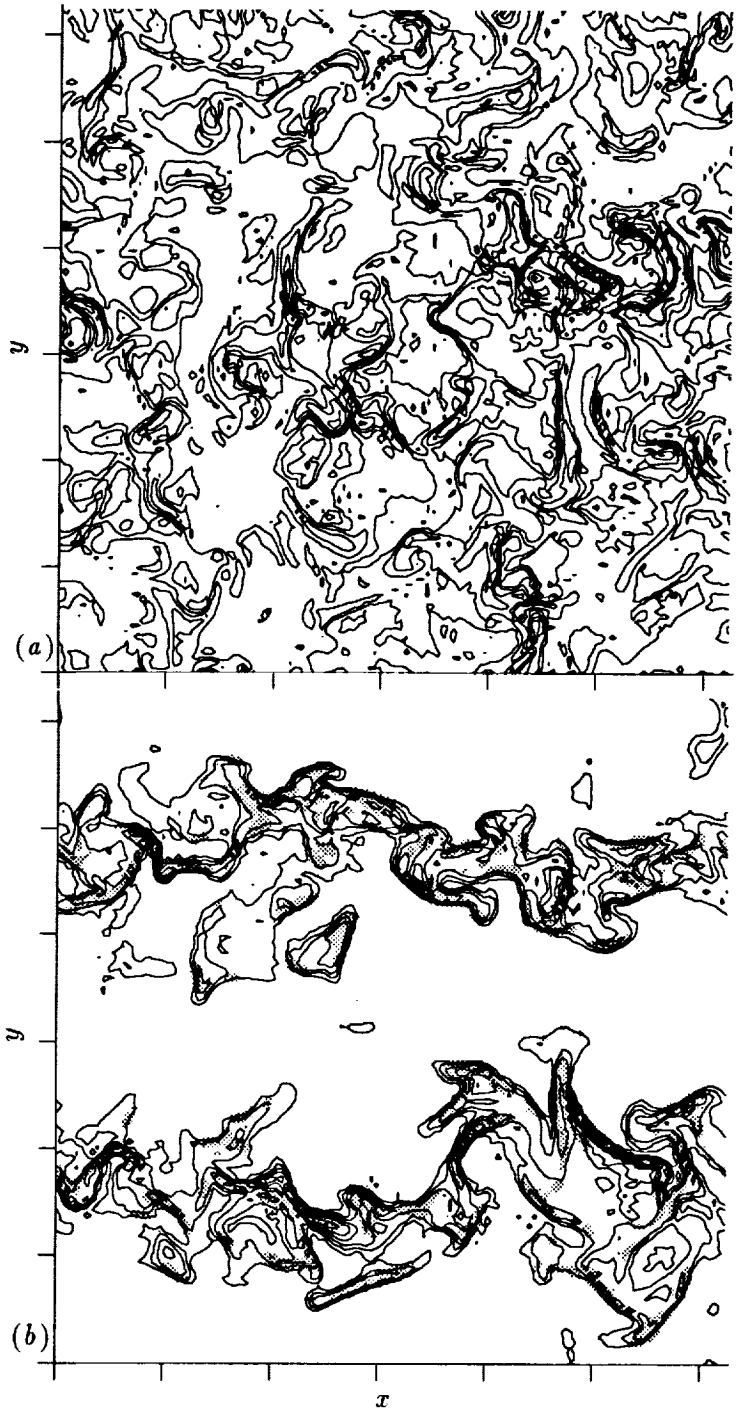

FIGURE 1. Scalar $\phi_A\phi_B$ (reaction rate over k) in an x–y plane at $t\epsilon/q^2 = 0.968$ for (a) blob initial conditions and (b) slab initial conditions. Contour increments are (a) 0.05 and (b) 0.1. Shaded areas indicate large values of the gradient amplification rate ($\psi_{Ai}e_{ij}\psi_{Bj} > 3.0\langle\psi_{Ai}e_{ij}\psi_{Bj}\rangle$).

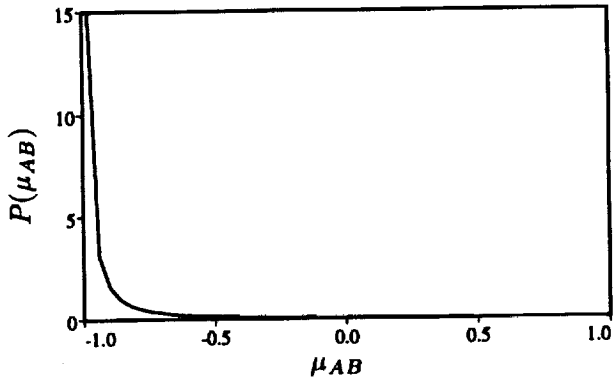

FIGURE 2. PDF of the cosine of the angle between ψ_A and ψ_B at $t\epsilon/q^2 = 0.497$ for the blob case ($\mu_{AB} = \psi_{Ai}\psi_{Bi}/(|\psi_A||\psi_B|)$).

including reversible reactions and the temperature-dependent kinetics. In addition, the alignment of reactant gradients with temperature gradient, the reaction product gradient, and the conserved scalar ($\phi_A - \phi_B$) gradient was considered. The results pertinent to this study are summarized here:

1. If $\mu_{AB}(t = 0) = -1$ (gradients initially aligned and opposed in the non-premixed system) then $\mu_{AB}(t)$ remains equal to -1 (aligned), independent of the reaction rate and of the presence of products of reaction (in the reversible case) including temperature, independent of the diffusivities D_A and D_B (which may differ), and independent of the strain rate e_{ij}, except as noted below.
2. A stability analysis of the case described in (1) above shows that in nonisothermal systems, the reactant concentration gradients can become misaligned, depending on the Zeldovich number and on the direction of the temperature gradient with respect to ψ_A.
3. If $\mu_{AB}(0) \neq -1$ (gradients initially misaligned) then the irreversible reaction (1) tends to align the gradients of ϕ_A and ϕ_B.
4. As the reaction rate constant k in (2) becomes large, the reactants become segregated such that $\mu = -1$ on the reaction surface and undefined elsewhere.
5. The alignment of a reacting and non-reacting scalar, say ϕ_A and ϕ, is preserved as in (1) above and is not influenced by the reaction rate even if gradients are initially misaligned.

Thus, in the simple non-premixed reaction case considered here, the initial scalar gradients are aligned ($\mu_{AB} = -1$), and remain aligned for all time. This theoretical result was confirmed in the direct numerical simulations by examining the pdf of μ_{AB}, which is approximately a delta functions at -1 (see figure 2).

2.3 Fokker-Planck closure

A Fokker-Planck (FP) molecular mixing closure was developed by Fox (1992a) to describe the evolution of the joint scalar, scalar gradient pdf in a system of reacting

one-dimensional, random-sized lamellae. Numerical (Fox, 1992b) and theoretical (Sokolov and Blumen, 1991a, 1991b) studies of diffusion in such systems have shown that the joint pdf evolves to a bivariate independent Gaussian pdf. However, if the scalar and scalar gradient are initially correlated, the correlation diminishes at a rate on the order of the scalar dissipation rate suggesting that the scalar and scalar gradient cannot be treated as independent random variables. Fox (1992b) has shown that the FP closure captures the form of the joint pdf and the decay rate of the correlation function for diffusion in random-sized lamellae in the absence of turbulent stretching, and suggested a modification to the closure to include the effect of the latter. In the following subsections, the application and extension of this model to the reacting system under consideration is presented.

2.3.1 A single inert scalar

In the following derivation for an inert scalar, the diffusion is assumed to be locally one-dimensional, so that only the magnitude of the scalar gradient is relevant. In §2.3.2, the alignment results of §2.2 will allow this treatment to be extended to the reacting multiple scalar case. For a scalar ϕ and its gradient ψ, the modified FP closure can be expressed in terms of a pair of stochastic differential equations:

$$d\phi = \kappa^2 A_\phi(\phi,\psi)dt + \kappa B_\phi(\phi,\psi)dW_\phi(t), \tag{5}$$

$$d\psi = \kappa^2 A_\psi(\phi,\psi)dt + C_{\omega^*}\omega^*\psi dt + \kappa B_\psi(\phi,\psi)dW_\psi(t), \tag{6}$$

where A_ϕ, B_ϕ, A_ψ, and B_ψ are functions determined as in Fox (1992a), $C_{\omega^*}\omega^*\psi$ is the gradient stretching term suggested by Fox (1992b), ω^* is the turbulence relaxation rate defined by Pope & Chen (1990) (see (9) below), and

$$\kappa^2 = D\langle\psi^2\rangle/\langle\phi^2\rangle = 6D/\lambda_\phi^2. \tag{7}$$

The turbulence relaxation rate, ω^*, is a random variable defined in terms of the (random) pseudo-dissipation rate,

$$\epsilon^*(x,t) = \nu\frac{\partial u_i}{\partial x_j}\frac{\partial u_i}{\partial x_j}, \tag{8}$$

and the (nonrandom) turbulent kinetic energy, $q^2\rangle/2 = \langle u_i u_i\rangle/2$, as

$$\omega^*(x,t) = 2\epsilon^*(x,t)/q^2(t). \tag{9}$$

Pope and Chen (1990) have proposed a stochastic differential equation for ω^* whose coefficients are independent of ϕ and ψ, and which yields a limiting log-normal pdf for ω^* . The gradient stretching constant, C_{ω^*}, is assumed to be independent of the initial conditions.

The FP model can be used to derive equations for the moments of the scalar and its gradient. In particular for an inert scalar in isotropic turbulence, the exact equations for the variance of the scalar is

$$\frac{d\langle\phi^2\rangle}{dt} = -2D\langle\psi^2\rangle, \tag{10}$$

and, from the model, the scalar gradient variance is

$$\frac{d\langle\psi^2\rangle}{dt} = -2C_\psi D\frac{\langle\psi^2\rangle^2}{\langle\phi^2\rangle} + 2C_{\omega^*}\langle\omega^*\psi^2\rangle, \tag{11}$$

where C_ψ is a parameter in the definition of the functions A_ψ and B_ψ in (6). In the absence of turbulence ($\omega^* = 0$), the above equations are closed and constitute a two-equation model for the scalar energy and its dissipation rate. For this case, Fox (1992b) has found that $C_\psi = 3$ gives a good fit to the random-sized lamellae data and is required by the limiting form of $\langle\phi^2\rangle/\langle\psi^2\rangle$ predicted by theory (Sokolov and Blumen, 1991a). Note that if ω^* and ψ are uncorrelated, or if ω^* is nonrandom as is often assumed in pdf modeling studies, then $\langle\omega^*\psi^2\rangle = \langle\omega^*\rangle\langle\psi^2\rangle$ and the equations are again closed. In particular, if $\langle\omega^*\rangle$ is time-independent, the long-time asymptotic behavior of the variances (characterized by constant $\langle\psi^2\rangle/\langle\phi^2\rangle$) can be determined as

$$\frac{d\langle\phi^2\rangle}{dt} \to -\frac{2C_{\omega^*}}{C_\psi - 1}\langle\omega^*\rangle\langle\phi^2\rangle. \tag{12}$$

Note that the scalar rms decreases exponentially in the limit of large t and the rate is independent of D. Other molecular mixing closures for the scalar pdf, such as the LMSE model (Pope, 1985) usually take

$$\frac{d\langle\phi^2\rangle}{dt} = -C_\phi\langle\omega^*\rangle\langle\phi^2\rangle \tag{13}$$

with $C_\phi = 2.0$.

The FP closure discussed above extends standard scalar mixing models in two ways: (1) it models the scalar dissipation rate instead of assuming that λ_ϕ is constant, and (2) it treats the turbulence relaxation rate as a random variable so that, for example, regions in the flow with large ω^* will be correlated with regions of large scalar gradient and hence with increased mixing and reaction. Direct numerical simulations indicate that these qualitative features are characteristic of turbulent reacting flows (see Leonard and Hill, 1991 and §3).

2.3.2 Multiple reacting scalars

In the FP closure, multiple reactive scalars are handled by first considering an inert scalar ϕ with gradient ψ, which are governed by the stochastic differential equations (5) and (6). Let ϕ_α and ψ_α, $\alpha = 1, ..., N$, denote reactive scalars and their gradients, respectively, all with the same molecular diffusivity as ϕ, and with linearly dependent initial values; that is $\phi_\alpha(x, y, z, t = 0) = a_\alpha\phi(x, y, z, 0) + b_\alpha$, and $\psi_\alpha(x, y, z, 0) = a_\alpha\psi(x, y, z, 0)$. As discussed by Pope (1985), the molecular mixing model to be developed below must be linear in the scalars ϕ_α, so in the absence of source terms

$$\frac{\partial\phi_\alpha}{\partial t} = F(\phi,\psi)\phi_\alpha + G_i(\phi,\psi)\psi_{\alpha i} - \langle F(\phi,\psi)\phi_\alpha\rangle - \langle G_i(\phi,\psi)\psi_{\alpha i}\rangle, \tag{14}$$

where F and G_i are functions to be determined. Using the same arguments, it can be shown that a similar linearity property must hold for ψ_α. Moreover, when the source term is zero, $\phi_\alpha(x,y,z,t) = a_\alpha\phi(x,y,z,t) + b_\alpha$ and $\psi_\alpha(x,y,z,t) = a_\alpha\psi(x,y,z,t)$ for all t. The scalars thus remain correlated for all time, implying that the same two Wiener processes (W_ϕ and W_ψ) that appear in (5) and (6) must also appear in the equations for ϕ_α and ψ_α (Fox, 1992a). Equivalently, the multiple reactive scalar model can be formulated in terms of $d\phi$ and $d\psi$ as follows.

Assume that a local one-to-one differentiable mapping exists between ϕ and ϕ_α, namely $\phi_\alpha = \Phi_\alpha(\phi,t)$. Differentiation then leads to an expression for the time-derivative of Φ_α:

$$\frac{\partial\Phi_\alpha}{\partial t} = D\psi^2\frac{\partial^2\Phi_\alpha}{\partial\phi^2} + S_\alpha(\Phi_1,...,\Phi_N), \tag{15}$$

Given ϕ and ψ, (15) is closed; however, it cannot be conveniently solved using Monte Carlo methods.

It is interesting that the conditional moment closure (CMC) (Bilger 1991) employs a similar mapping equation:

$$\frac{\partial\Phi_\alpha}{\partial t} = D\langle\psi^2 \mid \phi\rangle\frac{\partial^2\Phi_\alpha}{\partial\phi^2} + S_\alpha(\Phi_1,...,\Phi_N), \tag{16}$$

where $D\langle\psi^2|\phi\rangle$ is the conditional scalar dissipation rate of the inert scalar given ϕ. The CMC mapping equation is closed given ϕ and results in a joint pdf for ϕ and ϕ_α with a 1-dimensional support (it falls on a curve in (ϕ,ϕ_i)-space). However, in the current formulation, the support will, in general, be 2-dimensional since each value of ψ will result in a separate curve in (ϕ,ϕ_i)-space. Mell *et al.* (1992) have solved the CMC mapping equation numerically for the reaction $A + B \rightarrow P$ with $D\langle\psi^2|\phi\rangle$ and the pdf of ϕ taken directly from DNS, and found good agreement with the joint pdf of ϕ and ϕ_A computed from the DNS data (the curve computed by CMC falls near the maximum of the joint pdf found by DNS). In addition, they found that the CMC results are insensitive to the functional form used for $D\langle\psi^2|\phi\rangle$, which suggests that the source term may dominate the diffusion term in the mapping equation. We therefore hope that the crude model used for this term below will be adequate.

In order to apply a Monte Carlo method, $d\phi_\alpha$ is written in terms of its partial derivatives:

$$d\phi_\alpha = \frac{\partial\Phi_\alpha}{\partial\phi}d\phi + \frac{\partial\Phi_\alpha}{\partial t}dt, \tag{17}$$

or substituting (15)

$$d\phi_\alpha = \frac{\partial\Phi_\alpha}{\partial\phi}d\phi + D\psi^2\left(\frac{\partial^2\Phi_\alpha}{\partial\phi^2}\right)dt + S_\alpha(\phi_1,...,\phi_N)dt. \tag{18}$$

In (18) the diffusion term (premultiplied by D) is zero if the source term is zero or linear. Also, if the source term is such that Φ_α is time invariant (e.g., an infinitely fast bimolecular reaction) the sum of the diffusion and source terms is zero. Otherwise it must be closed in terms of the ϕ, ψ, ϕ_α and ψ_α, and the closure must be

linear in ϕ_α and ψ_α as discussed above. The simplest closure hypothesis is to assume that this term is independent of the modeled variables, leading to the simplest model of the form (14):

$$d\phi_\alpha = \frac{\partial \Phi_\alpha}{\partial \phi} d\phi - \langle \frac{\partial \Phi_\alpha}{\partial \phi} d\phi \rangle + S_\alpha(\phi_1, ..., \phi_N) dt. \tag{19}$$

The terms involving $\partial \Phi_\alpha / \partial \phi$ are closed in terms of ψ_α (see below).

To obtain a similar expression for $d\psi_{\alpha_i}$, note that our assumed form for ϕ_α implies that

$$\psi_{\alpha i} = \frac{\partial \phi_\alpha}{\partial x_i} = \frac{\partial \Phi_\alpha}{\partial \phi} \psi_i \tag{20}$$

The total derivative of $\psi_{\alpha i}$ is thus

$$d\psi_{\alpha i} = \frac{\partial^2 \Phi_\alpha}{\partial \phi^2} \psi_i \, d\phi + \frac{\partial \Phi_\alpha}{\partial \phi} \, d\psi_i + \frac{\partial^2 \Phi_\alpha}{\partial t \partial \phi} \psi_i \, dt. \tag{21}$$

The time derivative term can be evaluated by differentiating (15) with respect to x_i to obtain

$$\psi_i \frac{\partial^2 \Phi_\alpha}{\partial t \partial \phi} = D \frac{\partial^3 \Phi_\alpha}{\partial \phi^3} \psi^2 \psi_i + D \frac{\partial^2 \Phi_\alpha}{\partial \phi^2} \frac{\partial \psi^2}{\partial x_i} + \sum_\beta \frac{\partial S_\alpha}{\partial \phi_\beta} \frac{\partial \Phi_\beta}{\partial \phi} \psi_i \tag{22}$$

which when substituted into (21) yields

$$\begin{aligned} d\psi_{\alpha i} = & \frac{\partial^2 \Phi_\alpha}{\partial \phi^2} \psi_i \, d\phi + \frac{\partial \Phi_\alpha}{\partial \phi} \, d\psi_i \\ & + D \frac{\partial^3 \Phi_\alpha}{\partial \phi^3} \psi^2 \psi_i \, dt + D \frac{\partial^2 \Phi_\alpha}{\partial \phi^2} \frac{\partial \psi^2}{\partial x_i} \, dt + \sum_\beta \frac{\partial S_\alpha}{\partial \phi_\beta} \frac{\partial \Phi_\beta}{\partial \phi} \psi_i \, dt \end{aligned} \tag{23}$$

Terms involving more than one derivative of Φ_α are not closed with respect to ϕ_α and ψ_α. The first term is modeled as zero, which is exact if S_i is zero or linear and the diffusion terms are modeled as in (19) yielding

$$d\psi_{\alpha i} = \frac{\partial \Phi_\alpha}{\partial \phi} \, d\psi_i - \langle \frac{\partial \Phi_\alpha}{\partial \phi} \, d\psi_i \rangle + \sum_\beta \frac{\partial S_\alpha}{\partial \phi_\beta} \frac{\partial \Phi_\beta}{\partial \phi} \psi_i \, dt \tag{24}$$

The functional form of $\psi_{\alpha i}$ in (20) implies that all the scalar gradients are aligned with the gradient of the inert scalar ϕ, in agreement with the analysis in §2.2. Therefore, it is not necessary to treat ψ_α and ψ as vectors. Without loss of generality we can let $\psi_\alpha = \psi_{\alpha i} \psi_i / |\psi|$ (the projection of ψ_α onto the ψ direction) and $\psi = |\psi|$. This is also consistent with the one-dimensional nature of the FP model for the inert scalar (equations (5) and (6)). It is also clear that $\partial \Phi_\alpha / \partial \phi = \psi_\alpha / \psi$. With these simplifications the final model equations for the evolution of ϕ_α and ψ_α are

$$\frac{\partial \phi_\alpha}{\partial t} = \frac{\psi_\alpha}{\psi} \frac{\partial \phi}{\partial t} - \langle \frac{\psi_\alpha}{\psi} \frac{\partial \phi}{\partial t} \rangle + S_\alpha(\phi_1, ..., \phi_N) \tag{25}$$

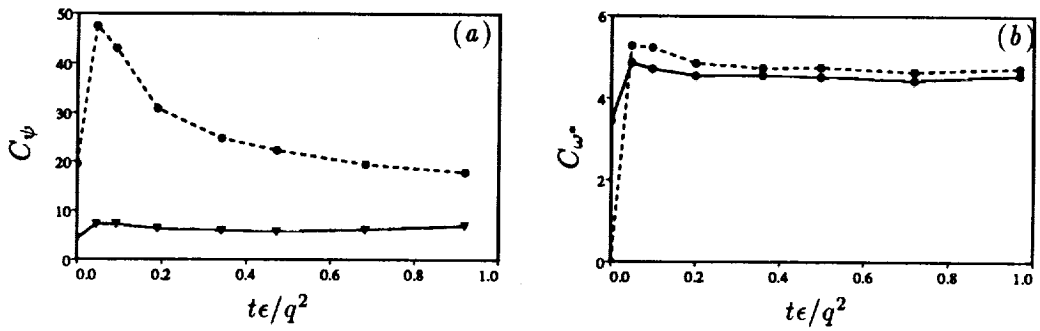

FIGURE 3. Evolution of the model constants (*a*) C_ψ and (*b*) C_{ω^*} in the direct numerical simulation for —— blob initial conditions and ---- slab initial conditions.

$$\frac{\partial \psi_\alpha}{\partial t} = (\frac{1}{\psi}\frac{\partial \psi}{\partial t})\psi_\alpha - \langle \frac{\psi_\alpha}{\psi}\frac{\partial \psi}{\partial t}\rangle + \sum_\beta \frac{\partial S_\alpha}{\partial \phi_\beta}\psi_\beta, \tag{26}$$

which in the absence of source terms are linear as required.

Since the marginal pdfs of ψ and ψ_α are both symmetric about zero, the expected value of ψ obtained from (26) should be zero for all time. The FP closure for ψ_α is similar to the LMSE closure since, in the absence of source terms, $\partial \ln|\psi_\alpha|/\partial t = \partial \ln|\psi|/\partial t$. But since $\partial \ln|\psi|/\partial t$ is not constant, the two closures are not identical; in particular, with the FP closure the joint pdf of ϕ and ψ evolves to a bivariate Gaussian (Fox, 1992a).

The FP closure can be extended to scalars with nonequal molecular diffusivities by including a separate inert scalar with the same molecular diffusivity as each corresponding reactive scalar. The stochastic differential equations for the new inert scalars have the same form as Eqs. (5) and (6) except with κ^2 modified to include the correct molecular diffusivity. The same Wiener processes (W_ϕ and W_ψ) must appear in each pair of stochastic differential equations as discussed by Fox (1992a).

2.4 Evaluation of model constants

The FP closure has two "universal" constants C_ψ and C_{ω^*} whose values can be determined using DNS data. The exact equations for an inert scalar and the magnitude of its gradient in a three-dimensional flow are

$$\frac{D\phi}{Dt} = D\nabla^2\phi, \tag{27}$$

$$\frac{D\psi^2}{Dt} = 2D\psi_i\frac{\partial^2\psi_i}{\partial x_j \partial x_j} - 2\psi_i e_{ij}\psi_j, \tag{28}$$

where e_{ij} is the strain rate tensor. By comparing the expected value of (28) with (11) derived from the FP model, the model constants can be evaluated as

$$C_{\omega^*} = -\frac{\langle \psi_i e_{ij}\psi_j\rangle}{\langle \omega^*\psi^2\rangle}, \tag{29}$$

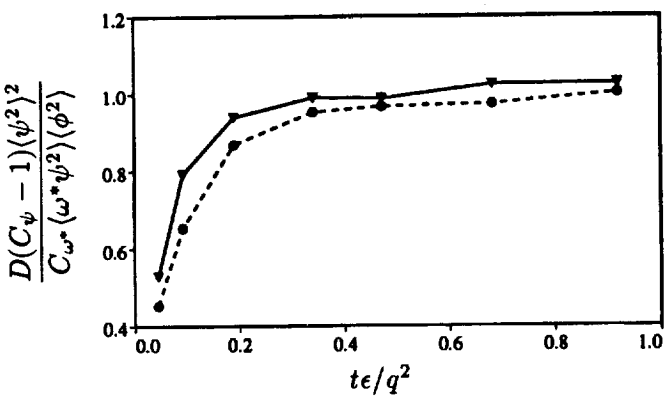

FIGURE 4. Evolution of $\frac{D(C_\psi-1)\langle\psi^2\rangle^2}{C_{\omega^*}\langle\omega^*\psi^2\rangle\langle\phi^2\rangle}$ evaluated from DNS for —— blob and ---- slab initial conditions.

and

$$C_\psi = -\frac{\langle\psi_i\nabla^2\psi_i\rangle\langle\phi^2\rangle}{\langle\psi^2\rangle^2}. \tag{30}$$

The model constants, evaluated from the direct numerical simulations using (29) and (30), are shown as functions of time in figure 3. It is clear from figure 3a that the gradient mixing constant, C_ψ, depends strongly on initial conditions. For the anisotropic slab initial conditions, C_ψ decreases steadily with time after an initial jump. On the other hand, for the isotropic blob initial conditions, $C_\psi \approx 6.7$ for all time. This difference is most likely due the difference in integral length scales of the scalar fields in the two cases. Integral length scale effects have not yet been incorporated into the FP closure, but have been shown to have a significant effect on the scalar dissipation rate (Eswaran and Pope, 1988; Eswaran and O'Brien, 1989; Kosály, 1989; Jiang and O'Brien, 1991). For the slab case, scalar integral length scales are initially infinite in two directions and decrease as the turbulent advection creates a more isotropic field. For the blob case, the integral length scale is approximately constant for all time. In contrast, the gradient stretching constant, C_{ω^*}, shown in figure 3b appears to be independent of initial conditions and approximately equal to 4.7 for all time.

An expression relating C_ψ and C_{ω^*} can be found from the limiting value of $\lambda_\phi^2 = 6\langle\phi^2\rangle/\langle\psi^2\rangle$. From Eqs. (10) and (11) for the FP model, the following relation is found for λ_ϕ^2:

$$\frac{d\lambda_\phi^2}{dt} = 12D(C_\psi - 1) - 2C_{\omega^*}\frac{\langle\omega^*\psi^2\rangle}{\langle\psi^2\rangle}\lambda_\phi^2. \tag{31}$$

For statistically stationary ω^*, (31) has a single stable limiting solution:

$$\lambda_\phi^2/6 = \frac{\langle\phi^2\rangle}{\langle\psi^2\rangle} = \frac{D(C_\psi-1)\langle\psi^2\rangle}{C_{\omega^*}\langle\omega^*\psi^2\rangle}. \tag{32}$$

Thus, if the model has asymptotic behavior consistent with the DNS, we should find that

$$\frac{D(C_\psi - 1)\langle\psi^2\rangle^2}{C_{\omega^*}\langle\omega^*\psi^2\rangle\langle\phi^2\rangle} \to 1 \tag{33}$$

for large t. The left side of (33) is plotted as a function of time in figure 4 for both the slab and blob cases. For both cases this quantity does indeed approach 1.

Mantel and Borghi (1991) have proposed a two-equation model for scalar energy, scalar dissipation similar in form to (10) and (11) but with $\langle\omega^*\rangle\langle\psi^2\rangle$ in place of $\langle\omega^*\psi^2\rangle$. In their model, the coefficients are defined in terms of a turbulence Reynolds number $Re_t = \sqrt{(q^2/2)}l_t/\nu$ so that, for large Re_t, $C_\psi = \beta_0\sqrt{Re_t}/2$, and $C_{\omega^*} = \alpha_0\sqrt{Re_t}/2$, with $\alpha_0 = 0.9$ and $\beta_0 = 1.25$ found by DNS (Borghi *et al.*, 1992). For $Re_t = 194$ of the present DNS simulations, these expressions yield $C_\psi = 8.7$ and $C_{\omega^*} = 6.3$. These estimates are both 30% larger than the values given above, implying that the ratio C_ψ/C_{ω^*} is similar. Since $C_\psi = 3$ in the limit where $Re_t = 0$ (Fox, 1992b), the Reynolds number dependence embodied in these large-Re_t relations may not be valid for these relatively low Reynolds number DNS computations. (Although the Re_t values for the DNS runs used to determine α_0 and β_0 have not yet appeared in the literature (Borghi *et al.*, 1992), they must be small due to the limitations of DNS.) This fact may explain some of the discrepancies between the two sets of values for the model constants.

2.5 Application to the single-step reaction

The FP closure described above has been used to generate joint pdfs of the reactant concentrations and their gradients for the 2-component, single-step reaction scheme (1) using a Monte Carlo simulation. For this reaction (25) and (26) yield:

$$d\phi_A = \frac{\psi_A}{\psi}d\phi - \langle\frac{\psi_A}{\psi}d\phi\rangle - k\phi_A\phi_B dt, \tag{34}$$

$$d\phi_B = \frac{\psi_B}{\psi}d\phi - \langle\frac{\psi_B}{\psi}d\phi\rangle - k\phi_A\phi_B dt, \tag{35}$$

$$d\psi_A = \frac{\psi_A}{\psi}d\psi - \langle\frac{\psi_A}{\psi}d\psi\rangle - k\phi_A\psi_B dt - k\phi_B\psi_A dt, \tag{36}$$

and

$$d\psi_B = \frac{\psi_B}{\psi}d\psi - \langle\frac{\psi_B}{\psi}d\psi\rangle - k\phi_A\psi_B dt - k\phi_B\psi_A dt. \tag{37}$$

The Monte Carlo algorithm uses fractional time-stepping to split the mixing and reaction steps into separate processes (Pope, 1985; Fox, 1992a). The expected values appearing in (34)–(37) are computed during the mixing step so that the mean values of the scalars and scalar gradients are constant during mixing. A constant turbulence relaxation rate, $\omega^* = \langle\omega^*\rangle$ was used in (6). The resulting joint pdf's are compared to the DNS results below.

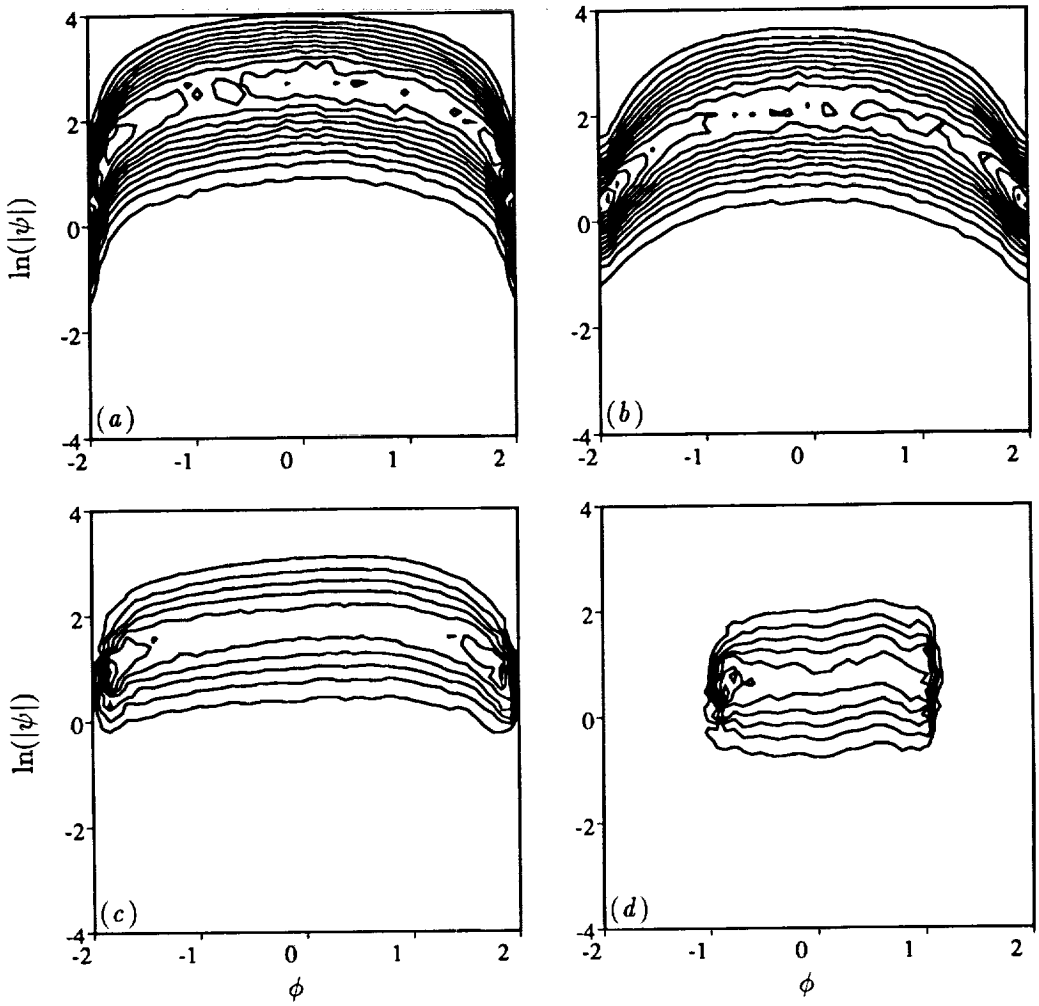

FIGURE 5. Conditional PDF of $\ln(|\psi|)$ given ϕ ($P(\ln(|\psi|) \mid \phi)$) for the direct numerical simulation with (a,b) slab initial conditions and (c,d) blob initial conditions at (a,c) $t\epsilon/q^2 = 0.497$ and (b,d) $t\epsilon/q^2 = 0.968$. At these times $\phi_{\rm rms}/\phi_{\rm rms}(t=0)$ is (a) 0.846, (b) 0.645, (c) 0.426, and (d) 0.172.

3. Results

3.1 Statistics of the inert scalar field

The DNS data have been used to compute a wide range of statistics involving the inert and reactive scalars and the magnitudes of their gradients. The marginal pdf $P(\phi)$ for the inert scalar is nearly identical in shape, at a given rms value, to those reported in previous DNS studies. The marginal pdf of the log of the magnitude of the inert scalar gradient, $P(\ln|\psi|)$, approaches a nearly Gaussian form, but with a slightly longer negative tail, in agreement with the DNS results of Eswaran and Pope (1988).

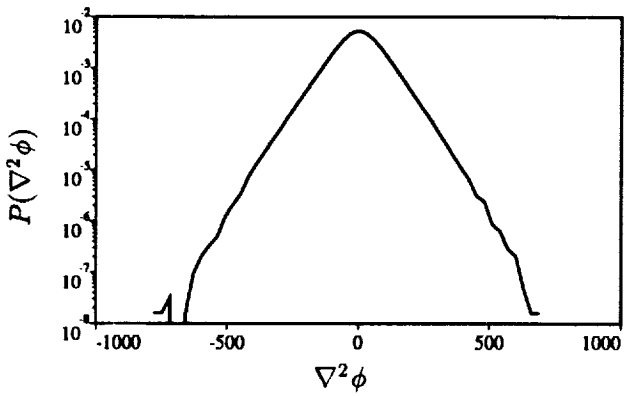

FIGURE 6. PDF of $\nabla^2\phi$ for the DNS with blob initial conditions at $t\epsilon/q^2 = 0.968$.

Of greater interest is the joint pdf of the inert or conserved scalar, ϕ, and its gradient, ψ, which has been the subject of both theory (Bilger, 1976; Fox, 1992a, 1992b; Gao and O'Brien, 1991; Meyers and O'Brien, 1981; Valiño and Dopazo, 1991) and experiments (Anselmet and Antonia, 1985). In most reactive mixing closures (e.g., the flamelet model), ϕ and ψ are assumed to be independent so that the joint pdf is separable, $P(\phi,\psi;t) = P(\phi;t)P(\psi;t)$. In order to check for independence using the DNS data, the conditional pdf of ψ given ϕ, defined by $P(\psi|\phi;t) = P(\phi,\psi;t)/P(\phi;t)$, has been computed. Note that if ϕ and ψ are independent, then $P(\psi|\phi;t) = P(\psi;t)$ and will thus be independent of ϕ. Examples of the computed conditional pdf are shown in figure 5. From figure 5a ($\phi_{\rm rms}/\phi_{\rm rms}(t = 0) = 0.846$) it can be seen that near the start of the molecular mixing process, the scalar and scalar gradient are correlated. The correlation decays slowly so that in figure 5b ($\phi_{\rm rms}/\phi_{\rm rms}(0) = 0.645$) the conditional pdf continues to show a important ϕ-dependence. Not until the molecular mixing process is farther along ($\phi_{\rm rms}/\phi_{\rm rms}(0) = 0.172$) as shown in figure 5d does the conditional pdf appear to be independent of ϕ.

Another interesting pdf is that of the Laplacian of ϕ shown in figure 6 on a log-linear plot for $\phi_{\rm rms}/\phi_{\rm rms}(0) = 0.172$. As is clear from the form of the pdf, it is non-Gaussian with nearly exponential tails over 4 decades.

9.2 Statistics for inert scalar mixing

Statistics involving the scalar or scalar gradient and various turbulence quantities have been computed using the DNS data. For example, the scalar gradient-turbulence relaxation rate correlation function, defined by

$$\frac{\langle\omega^*\psi^2\rangle}{\langle\omega^*\rangle\langle\psi^2\rangle} - 1, \tag{38}$$

was found to be approximately time independent with values of 0.06 for the blob case and 0.15 for the slab case, indicating that ω^* and ψ^2 have a slight tendency to be simultaneously larger than their mean value. This tendency can be seen

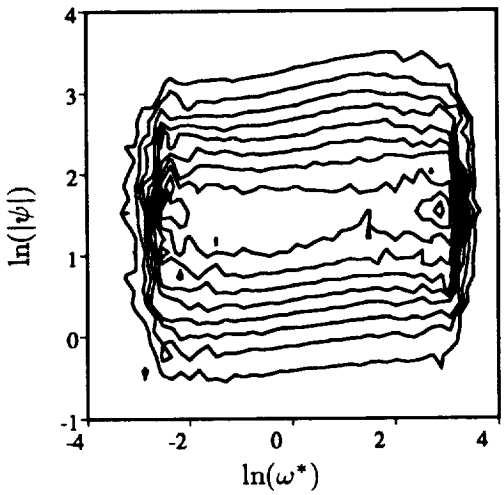

FIGURE 7. Conditional pdf of $\ln(|\psi|)$ given $\ln(\omega^*)$ for the DNS with slab initial conditions at $t\epsilon/q^2 = 0.968$.

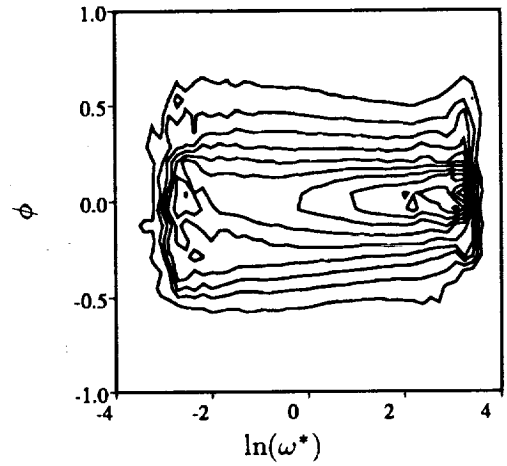

FIGURE 8. Conditional pdf of ϕ given $\ln(\omega^*)$ for the DNS with blob initial conditions at $t\epsilon/q^2 = 0.968$.

more clearly by examining the conditional pdf of $\ln(|\psi|)$ given $\ln(\omega^*)$ shown in figure 7 (slab case with $\phi_{\rm rms}/\phi_{\rm rms}(0) = 0.645$). From this figure it can be seen that the conditional pdf has a nearly constant shape but shifts upward as $\ln(\omega^*)$ increases. This behavior is consistent with the FP closure (6) wherein ω^* appears as a stretching (positive) term in the drift coefficient.

Similar conclusions can be drawn from the conditional pdf of ϕ given $\ln(\omega^*)$ shown in figure 8 for the blob case at $\phi_{\rm rms}/\phi_{\rm rms}(0) = 0.172$. There it can be seen that larger values of $\ln(\omega^*)$ lead to smaller conditional variances for ϕ. This is consistent with the model equations in that large $\ln(\omega^*)$ leads to large gradients and hence

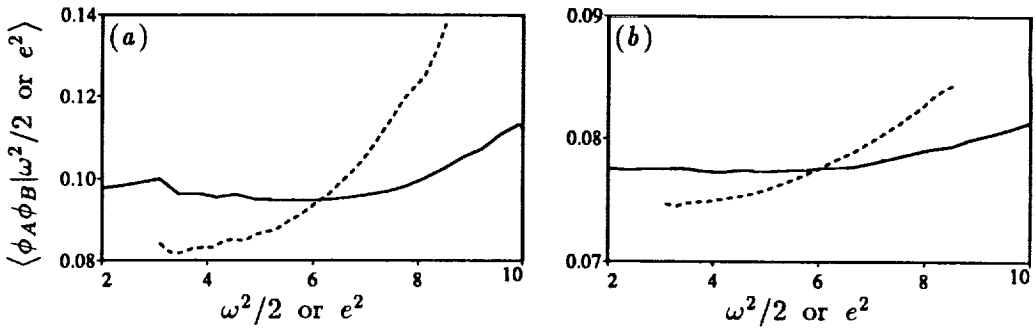

FIGURE 9. Conditional expectation of $\phi_A \phi_B$ (reaction rate over k) given —— enstrophy (ω^2) and ---- dissipation (e^2) for (a) slab initial conditions and (b) blob initial conditions at $t\epsilon/q^2 = 0.968$.

faster scalar dissipation.

Finally, as noted by Pope and Chen (1990), the DNS simulations confirm that the log of the pseudo-dissipation rate of the turbulence, $\ln \epsilon^*$ is more nearly Gaussian than is the log of the true turbulence dissipation rate, $\ln \epsilon$. For example, the skewness and flatness of $\ln \epsilon^*$ are -0.06 and 3.05, respectively, compared to -0.29 and 3.24 for $\ln \epsilon$ at $t\epsilon/q^2 = 0.968$

3.3 Statistics of reacting scalars

Some statistical quantities evaluated in previous simulations in decaying turbulence at lower Reynolds numbers (Leonard *et al.* 1988, Leonard & Hill 1988, 1990, 1992) and in a similar study for a non-reacting system (Nomura & Elgobashi 1992) were examined in order to determine the extent to which the present system exhibits the same physical behavior. For example, pdf's of the cosine between the directions of the reactant scalar gradients and the eigenvectors of the strain rate tensor, and plots of the eigenvectors superposed on reaction rate contours, show that there is considerable tendency for the most compressive eigenvector to align with the scalar gradients and to lie across the reaction zone. Furthermore, there is a similar but less pronounced tendency for the intermediate strain rate eigenvector to lie tangent to the reaction zones and isoscalar surfaces.

Figures 9 and 10 show the effect of certain kinematic quantities on the reaction rate, and *vice versa*, at t=0.92. In figure 9, for reaction rate conditioned on levels of strain and enstrophy, $\langle \phi_A \phi_B \mid e^2 \rangle$ and $\langle \phi_A \phi_B \mid \omega^2/2 \rangle$ where $e^2 = e_{ij} e_{ij}$, it is seen that strain has a marked effect on reaction rate, but the effect of vorticity is considerably less. The converse plot, figure 10 for strain and enstrophy conditioned on reaction rate, confirms the previous observation of Leonard & Hill (1990) that conditional averages of e^2 and $\omega^2/2$ are near their volume averages and each other, except for the regions of most intense reaction rate where the straining is very high and the enstrophy is appreciably less than the volume averaged value.

Regions where the gradient amplification term, $\langle \psi_{Ai} e_{ij} \psi_{Bj} \rangle$, is greater than $3.0 \langle \psi_{Ai} e_{ij} \psi_{Bj} \rangle$ are shaded in figure 1b. Clearly the largest values of this term are associated with peak values in the reaction rate, supporting earlier claims by

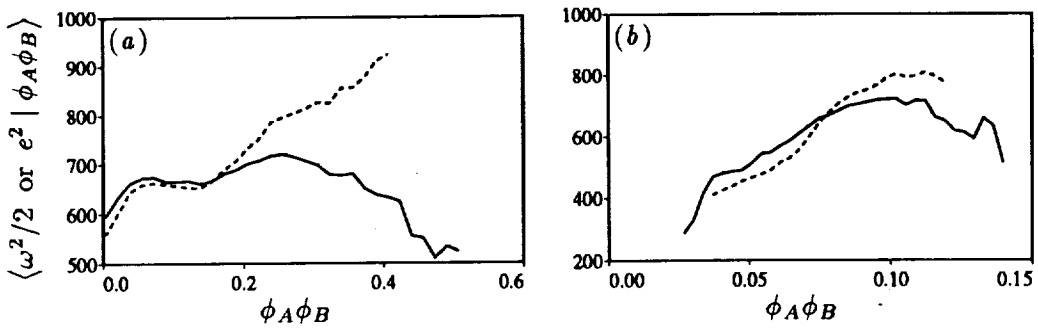

FIGURE 10. Conditional expectation of —— enstrophy (ω^2) and ---- dissipation (e^2) given $\phi_A\phi_B$ (reaction rate over k) for (a) slab initial conditions and (b) blob initial conditions at $t\epsilon/q^2 = 0.968$.

Leonard & Hill (1990, 1992) and underlining the importance of the modeled gradient amplification term in the FP model. Although not shown, the gradient amplification term seldom takes on negative values and since ψ_A and ψ_B tend to be aligned and opposing in the reaction zone, the compressive part of e_{ij} must dominate this term as expected.

Finally, various scalar gradient-strain rate correlation coefficients important in mixing studies were evaluated. One such quantity, $\langle \psi_{Ai} e_{ij} \psi_{Bj} \rangle / \langle \psi_{Ai} \psi_{Bi} \rangle \sqrt{e^2}$, approaches the value -0.45 for the slab case and -0.40 for the blob case; the same values are obtained for the conserved or inert scalar ϕ in these two cases. These values differ somewhat from the values -0.56 and -0.45 (-0.52 and -0.43 for the nonreacting scalars) found in decaying turbulence by Leonard & Hill (1990) and the value -0.5 found by Kerr (1985) for a nonreacting scalar in forced turbulence.

The joint pdf of the reacting scalars, ϕ_A and ϕ_B have also been computed using the DNS data and can be compared to the joint pdf found from the FP closure. For example, the joint pdf at $\phi_{\text{rms}}/\phi_{\text{rms}}(0) = 0.426$ is shown in figure 11 and that found using the FP closure for the same value of $\phi_{\text{rms}}/\phi_{\text{rms}}(0)$ in figure 12a. It can be seen that, despite the closure approximations needed to derive (19) and (24), the general shape of the pdf predicted by the FP closure corresponds closely to that found by DNS. In particular, the width of the curved region of significant probability is about the same in the DNS and the model. †

The comparisons between the pdfs of the modeled and DNS gradients (figures 11(b-d) and 12(b-d)) are not nearly as good, though the modeled gradients do have the correct order of magnitude. The strange bimodal structure of the gradient–gradient pdf (figure 12d) is presumably caused by one of the modeling assumptions used to derive equation (24).

† This can also be compared to the CMC model which predicts no scatter about the curve (Riley, 1992).

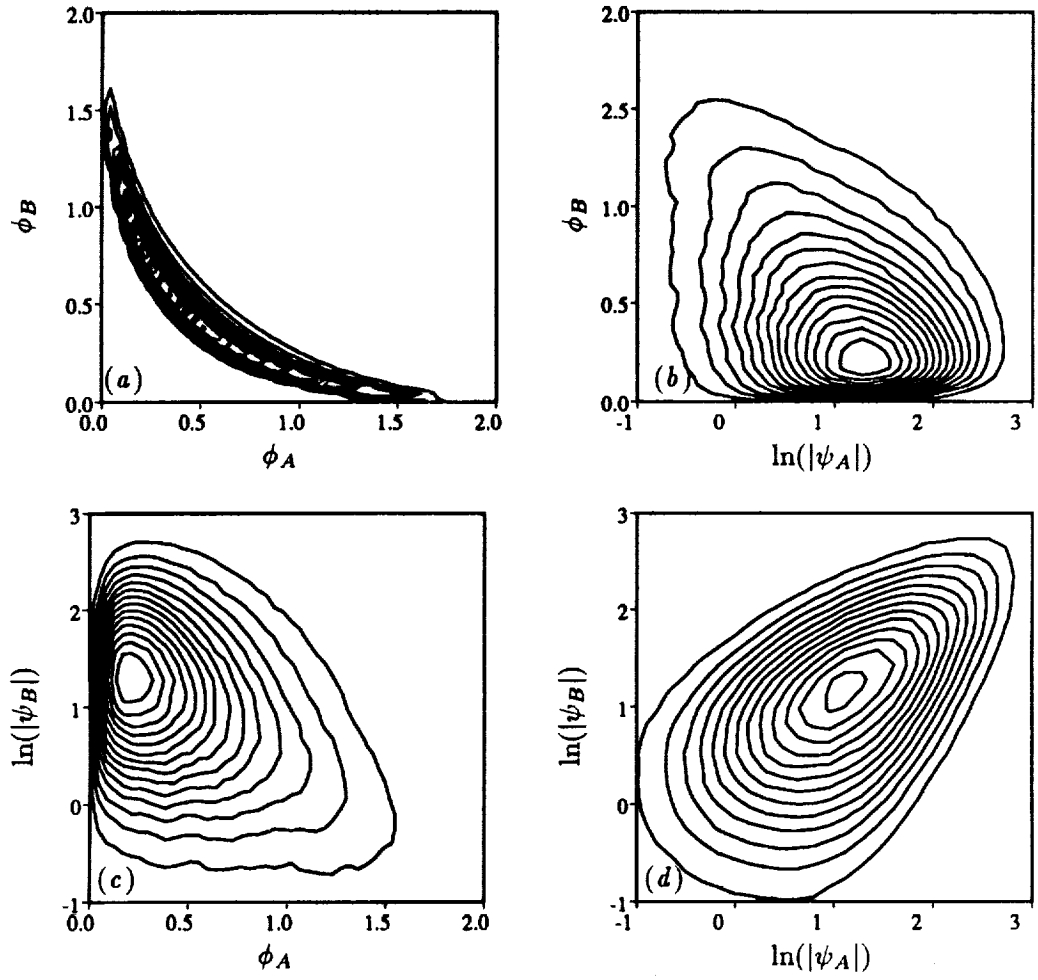

FIGURE 11. Joint pdf's of reactant concentrations and gradients from the DNS for blob initial conditions at $t\epsilon/q^2 = 0.497$.

4. Conclusions

Direct numerical simulations of a single-step chemical reaction between non-premixed reactants in forced isotropic turbulence were made for both "slab" and "blob" initial scalar reactant configurations. As found in previous simulations at lower Reynolds number, the amplification of concentration gradients in the reaction zone by the strain field was seen to be an important feature of these flows, in that regions of large local reaction rate are coincident with regions of large values of the gradient amplification factor.

An analysis of the alignment of various scalar gradients with each other provides some justification for treating the mixing process as locally one-dimensional as assumed in the Fokker-Planck model studied here and other closures.

Comparisons were made between predictions of the FP closure and results of

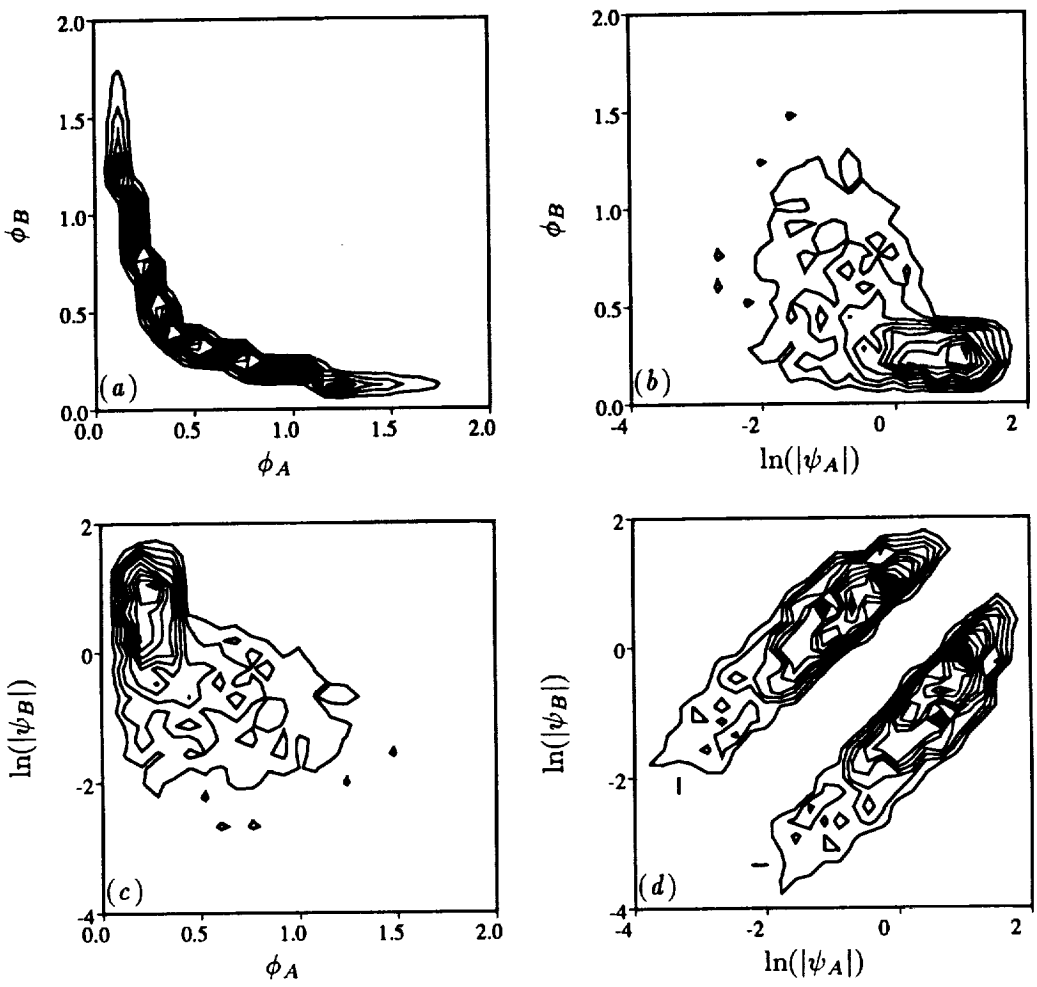

FIGURE 12. Joint pdf's of reactant concentrations and gradients from the FP model for the same conditions as in figure 11.

turbulence simulations. The closure's treatment of gradient stretching as a bilinear term in the model equation is generally supported by the DNS data. For example, the gradient stretching constant was found to be independent of initial conditions, and the DNS results for the joint pdf of the scalar gradient and the turbulence relaxation rate were found to be consistent with the model. Likewise, the closure's prediction for the joint pdf of the reactive scalars is very similar in shape to the DNS result. However, it was also found that for the non-isotropic initial scalar field the gradient mixing constant appearing in the closure is not constant as assumed, and that the closure's prediction for the form of the joint reactive scalar gradient pdf differs significantly from the DNS result. The former can most likely be accounted for in the closure by incorporating scalar integral length scale information, and the latter by modifying the closure assumptions used in deriving (24) from (23). In any

case, since it can be easily incorporated into existing Monte-Carlo simulation codes (Pope, 1985), the formulation of the FP closure in terms of a stochastic process offers a significant computational advantage over other closures that require the solution of a reaction-diffusion equation.

Acknowledgments

Authors ROF and JCH appreciate the generous support and use of the facilities provided by the Center for Turbulence Research. Portions of the work of ROF were supported by NSF Grant CTS-9158124. The authors appreciate the use of data from a high resolution simulation by R. S. Rogallo and A. A. Wray for forced, homogeneous turbulence, and also appreciate helpful dialogs with L. Vervisch, T. Poinsot, A. Trouvé, and S. Mahalingam.

REFERENCES

ANSELMET, F. & ANTONIA, R. A. 1985 Joint statistics between temperature and its dissipation in a turbulent jet. *Phys. Fluids.* **28,** 1048–1054.

BILGER, R. W. 1976 Turbulent jet diffusion flames. *Prog. Energy Combust. Sci.* **1,** 87–109.

BILGER, R. W. 1991 Conditional moment methods for turbulent reacting flows using Crocco variable conditions. *Charles Kolling Research Lab. TN F-99* (Dept. Mech. Eng., The Univ. of Sydney)

BORGHI, R., DOPAZO, C., MANTEL, T. &PICART, A. 1992 The modeling of the scalar dissipation rate in turbulent mixing. (In preparation.)

CHEN, H. C., CHEN, S., & KRAICHNAN, R. H. 1989 Probability distribution of a stochastically advected scalar field. *Phys. Rev. Lett.* **63,** 2657.

ESWARAN, V. & O'BRIEN, E. E. 1989 Simulations of scalar mixing in grid turbulence using an eddy-damped closure model. *Phys. Fluids A.* **1,** 537–548.

ESWARAN, V. & POPE, S. B. 1988 Direct numerical simulations of the turbulent mixing of a passive scalar. *Phys. Fluids.* **31,** 506–520.

FOX, R. O. 1992a The Fokker-Planck closure for turbulent molecular mixing: passive scalars. *Phys. Fluids A.* **4,** 1230–1244.

FOX, R. O. 1992b On the joint scalar, scalar gradient pdf in lamellar systems. *Phys. Fluids A* (submitted).

GAO, F. 1991 Mapping closure and non-Gaussianity of the scalar probability density function in isotropic turbulence. *Phys. Fluids A.* **3,** 2438.

GAO, F. & O'BRIEN, E. E. 1991 Joint probability density function of a scalar and its gradient in isotropic turbulence. *Phys. Fluids A.* **3,** 1625–1632.

JIANG, T. L. & O'BRIEN, E. E. 1991 Simulation of scalar mixing by stationary isotropic turbulence. *Phys. Fluids A.* **3,** 1612–1624.

KERR, R. M. 1985 Higher-order derivative correlations and the alignment of small-scale structures in isotropic numerical turbulence. *J. Fluid Mech.* **153,** 31–58.

KERSTEIN, A. 1991 Linear-eddy modeling of turbulent transport, Part VI. Microstructure of diffusive scalar mixing fields. *J. Fluid Mech.* **231,** 361–394.

KOSÁLY, G. 1989 Scalar mixing in isotropic turbulence. *Phys. Fluids A.* **1,** 758–760.

KOSÁLY, G. & GIVI, P. 1987 Combust. Flame. *70.* **101.**

LEONARD, A. D. & HILL, J. C. 1988 Direct numerical simulation of turbulent flows with chemical reaction. *J. Sci. Comput.* **3,** 25–43.

LEONARD, A. D. & HILL, J. C. 1990 Kinematics of the reaction zone in homogeneous turbulence. *Proc. 12th Sympos. Turb. (Rolla),* submitted for publication.

LEONARD, A. D. & HILL, J. C. 1991 Scalar dissipation and mixing in turbulent reacting flows. *Phys. Fluids A.* **3,** 1286–1299.

LEONARD, A. D. & HILL, J. C. 1992 Mixing and chemical reaction in sheared and nonsheared homogeneous turbulence. *Fluid Mech. Research.* **10,** 273–297.

LEONARD, A. D., HILL, J. C., MAHALINGAM, S., & FERZIGER, J. H. 1988 Analysis of homogeneous turbulent reacting flows. *Studying Turbulence Using Numerical Simulation Databases-II. Proceedings of the 1988 Summer Program* (Moin, P., Reynolds, W. C., & Kim, J., eds., Center for Turbulence Research Report **CTR-S88,**243–255.

MANTEL, T. & BORGHI, R. 1991 A new model of premixed wrinkled flame propagation based on a scalar dissipation equation. (preprint).

MELL, W. E., NIELSEN, V., KOSÁLY, G. & RILEY, J. J. 1992 Direct numerical simulation investigation of the conditional moment closure model for nonpremixed turbulent reacting flows. *Combust. Sci. Tech.* (in press).

MEYERS, R. E. & O'BRIEN, E. E. 1981 The joint pdf of a scalar and its gradient at a point in a turbulent fluid. *Combust. Sci. and Tech.* **26,** 123–134.

NOMURA, K. K. & ELGOBASHI, S. E. 1992 Mixing characteristics of an inhomogeneous scalar in isotropic and homogeneous sheared turbulence. *Phys. Fluids A.* **4,** 606–625.

O'BRIEN, E. E 1980 The probability density function (pdf) approach to reacting turbulent flows.. *Turbulent Reacting Flows* (Libby, P. A. and Williams, F. A., eds.) *Topics in Applied Physics.* **44,** Springer-Verlag, Heidelberg.

POPE, S. B. 1985 PDF methods for turbulent reactive flows. *Prog. Energy Combust. Sci.* **11,** 119–192.

POPE, S. B. & CHEN, Y. L. 1990 The velocity-dissipation probability density function model for turbulent flows. *Phys. Fluids A.* **2,** 1437–1449.

POPE, S. B. 1991 Mapping closures for turbulent mixing and reaction. *Theor. Comput. Fluid. Dyn.* **2,** 255.

RILEY, J. J. 1992 Investigation of closure models for turbulent reacting flows using direct numerical simulations. *19th Symp. on Turbulence,* Rolla, MO.

ROGALLO, R. S. 1981 Numerical experiments in homogeneous turbulence. *NASA TM 81315.*

SOKOLOV, I. M. & BLUMEN, A. 1991a Diffusion-controlled reactions in lamellar systems. *Phys. Rev. A.* **43,** 2714.

SOKOLOV, I. M. & BLUMEN, A. 1991b Distribution of striation thicknesses in lamellar systems. *Phys. Rev. A.* **43,** 6545.

VALIÑO, L. & DOPAZO, C. 1991 Joint statistics of scalars and their gradients in nearly homogeneous turbulence. *Advances in Turbulence.* **3** (Springer), 312–323.